Published in final edited form as:
Mol Cell. 2014 August 7; 55(3): 422–435. doi:10.1016/j.molcel.2014.05.012.

The Calcineurin Signaling Network Evolves Via Conserved Kinase–Phosphatase Modules That Transcend Substrate Identity

Aaron Goldman[#1], **Jagoree Roy**[#1], **Bernd Bodenmiller**[2], **Stefanie Wanka**[2], **Christian R. Landry**[3], **Ruedi Aebersold**[4,5], and **Martha S. Cyert**[1,#]

[1]Department of Biology, Stanford University, Stanford, CA 94305, USA [2]Institute of Molecular Life Sciences, University of Zürich, 8057 Zürich, Switzerland [3]Institut de Biologie Intégrative et des Systèmes, PROTEO, Département de Biologie, Université Laval, Québec G1V 0A6, Canada [4]Department of Biology, Institute of Molecular Systems Biology, ETH Zürich, 8093 Zürich, Switzerland [5]Faculty of Science, University of Zürich, 8057 Zürich, Switzerland

[#] These authors contributed equally to this work.

Summary

To define the first functional network for calcineurin, the conserved Ca^{2+}/calmodulin-regulated phosphatase, we systematically identified its substrates in *S. cerevisiae* using phosphoproteomics and bioinformatics, followed by co-purification and dephosphorylation assays. This study establishes new calcineurin functions and reveals mechanisms that shape calcineurin network evolution. Analyses of closely related yeasts show that many proteins were recently recruited to the network by acquiring a calcineurin-recognition motif. Calcineurin substrates in yeast and mammals are distinct due to network rewiring but surprisingly are phosphorylated by similar kinases. We postulate that co-recognition of conserved substrate features, including phosphorylation and docking motifs, preserves calcineurin-kinase opposition during evolution. One example we document is a composite docking site that confers substrate recognition by both calcineurin and MAPK. We propose that conserved kinase-phosphatase pairs define the architecture of signaling networks and allow other connections between kinases and phosphatases to develop and establish common regulatory motifs in signaling networks.

[#]Corresponding author mcyert@stanford.edu phone: (650) 723-9970 fax: (650) 724-9945.

Author Contributions

All authors contributed to experimental design. Interaction assays, Elm1 and network analyses performed by A.G. Dephosphorylation assays, Dig2 and Tda1 analyses performed by J.R. Mass spectrometry performed and analyzed by B.B. and S.W. Analysis of PxIxIT conservation guided by C.R.L. Manuscript written by A.G., J.R., and M.S.C.

Introduction

Cells respond to environmental changes through a complex network of regulatory circuits that often rely on the modulation of protein phosphorylation. Although the kinase and phosphatase cornerstones of these networks are highly conserved, the cues to which they respond and the targets they modulate change dramatically during evolution to accommodate new regulatory responses (Bhattacharyya et al., 2006; Moses and Landry, 2010; Sun et al., 2012). Elucidation of kinase signaling pathways and their rewiring has been greatly aided by global identification of kinase substrates, primarily through large-scale phosphoproteomic studies (Roux and Thibault, 2013). Because protein kinases phosphorylate characteristic motifs, their substrates can be predicted to some extent based on sequences surrounding the phosphorylated residue (Dinkel et al., 2012).

In contrast, less is known about phosphatase signaling due to challenges inherent to identification of their substrates (Bodenmiller et al., 2010; Breitkreutz et al., 2010; Fiedler et al., 2009; Hendrickx et al., 2009). First, phosphatases exhibit limited preference for the amino acids flanking a dephosphorylated residue; hence phosphorylation site sequences cannot be used to predict their targets (Li et al., 2013). Second, phosphatase substrates must be appropriately phosphorylated before dephosphorylation events can be detected. Consequently, both *in vivo* and *in vitro* analyses of phosphatase activity are dependent upon the activity of kinases that phosphorylate specific residues on the targets. We overcame these hurdles and developed a novel, systematic strategy to identify substrates of calcineurin (CN), the Ca^{2+}/calmodulin-dependent protein phosphatase. These studies uncovered new functions for CN in the model organism *Saccharomyces cerevisiae* and yielded surprising insights into the evolution of signaling networks.

CN is highly conserved, but regulates distinct processes in fungi and mammals. In mammals, CN dephosphorylates and activates the NFAT family of transcription factors during T-cell activation, cardiac hypertrophy, and development, and CN inhibitors are in wide clinical use as immunosuppressants (Safa et al., 2013). CN substrates also include components of synaptic vesicle endocytosis, ion channels, cytoskeletal and cell cycle regulators, and modulators that promote crosstalk between Ca^{2+}/CN and other signaling pathways. CN is highly abundant in the brain, where it regulates synaptic plasticity, and its misregulation is associated with Alzheimer's and Huntington's diseases, cancer, Down's syndrome, and schizophrenia (Cyert and Roy, 2013). In *S. cerevisiae* and other fungi, CN regulates a stress response that is essential for survival during a variety of stringent environmental conditions, including survival in a host for human fungal pathogens (Steinbach et al., 2007). A handful of CN substrates have been identified in yeast, including the CN-activated transcription factor, Crz1, and proteins that function in sphingolipid biosynthesis, protein trafficking and calcium homeostasis (reviewed in (Cyert and Philpott, 2013). To date, the CN regulator Rcn1/RCAN1 is the only orthologous CN substrate identified in both yeast and mammals (Kingsbury and Cunningham, 2000), suggesting that turnover in CN targets has allowed functional divergence of the enzyme in fungal and animal lineages.

CN, a heterodimer of a regulatory (CNB) and a catalytic (CNA) subunit, is activated when Ca^{2+}/calmodulin binds to CNA and disrupts an autoinhibitory domain – active site interaction (Cyert and Roy, 2013). Like other phosphatases, CN is highly selective for its targets but dephosphorylates sites with little sequence similarity (Donella-Deana et al., 1994; Li et al., 2013). Instead, CN primarily recognizes short, degenerate docking motifs, PxIxIT and LxVP, in its substrates that are distinct from sites of dephosphorylation (Roy and Cyert, 2009). Substrate engagement via these sites is critical for dephosphorylation and small molecules, FK506 and cyclosporine A, and the viral A238L protein effectively inhibit CN by preventing substrate binding rather than occluding the CN active site (Grigoriu et al., 2013; Rodriguez et al., 2009). During dephosphorylation, PxIxIT and LxVP motifs serve different functions: PxIxIT sites tether substrates to CN by extending a β-sheet in CNA (Li et al., 2007) and increase local substrate concentration, but are not essential for dephosphorylation (Aramburu et al., 1998; Aramburu et al., 1999). PxIxIT–CN interactions are low-affinity (15-250 μM), and changing this affinity alters the Ca^{2+}-dependence of substrate dephosphorylation *in vivo* (Roy et al., 2007). LxVP sites are thought to orient substrates during dephosphorylation (Grigoriu et al., 2013; Roy and Cyert, 2009). Both PxIxIT and LxVP motifs are difficult to identify due to degeneracy in their sequences and variable orientation and spacing relative to each other and sites of dephosphorylation. Thus, developing algorithms that effectively identify these sequences would greatly facilitate *de novo* identification of CN substrates.

There is growing appreciation for the importance of docking sequences and other short linear motifs (SLiMs), typically located in rapidly evolving, disordered protein domains, for determining both selectivity and modularity in signaling networks (Bhaduri and Pryciak, 2011; Davey et al., 2012; Won et al., 2011). Docking motifs mediate interaction of some kinases with substrates and regulators, and facilitate rewiring of these signaling pathways through their gain and loss (Bhattacharyya et al., 2006). In this study, we systematically identify CN substrates in yeast and show that gain and loss of PxIxIT docking sites drives evolutionary change in CN targets. We also demonstrate that a conserved group of protein kinases regulate CN substrates in fungi and mammals despite divergence in target identity. CN-kinase opposition may be preserved through recognition of phosphorylation site motifs and/or docking sites in substrates by both regulators, and contribute to the evolution of direct regulatory connections between kinases and phosphatases, which ultimately establish feed forward circuits and other common network regulatory motifs.

Results and Discussion

Strategy for identification of CN substrates

We developed a workflow to identify substrates for CN in the budding yeast *S. cerevisiae* by integrating *in vivo*, *in silico*, and *in vitro* analyses (Figure 1A). High confidence candidates were selected from the yeast proteome based on two criteria: 1) hyperphosphorylation in the absence of CN activity *in vivo* and 2) presence of putative PxIxIT docking sites based on sequence analysis *in silico*. Physical interaction with CN *in vivo* was assessed for each candidate to verify the presence of a CN docking site, and specific PxIxIT interaction was

confirmed in some cases. Finally, direct dephosphorylation by CN *in vitro* established substrates among the interacting proteins.

Characterization of the CN-dependent phosphoproteome

CN-dependent dephosphorylation events were identified by analyzing phosphorylated peptides in extracts of CN-deficient and CN-proficient yeast using quantitative, label-free mass spectrometry (refer to Experimental Procedures, Table S1). Strains chronically devoid of CN through deletion of the catalytic or regulatory subunits (*cna1*Δ *cna2*Δ and *cnb1*Δ, respectively) (Cyert and Philpott, 2013) were compared to WT and changes in WT cells induced by acute inactivation of CN with FK506 were also studied. Ca^{2+}/CN signaling was activated in all cases with extracellular $CaCl_2$ treatment.

In total, these three screens identified approximately 25% of yeast proteins as being phosphorylated; 4524 distinct phosphorylated peptides from 1350 proteins were detected in triplicate (4.8% FDR, Table S1). 660 phosphorylated peptides were significantly more abundant in extracts of CN-proficient cells, representing signaling events that CN impacts indirectly, e.g. by directly or indirectly activating kinases or inhibiting other phosphatases. More importantly, 699 phosphorylated peptides, representing 387 proteins, were significantly more abundant in a CN-deficient extract (Figure 1B, Figure S1A). Many of the same phosphorylated peptides were enriched in *cna1*Δ *cna2*Δ and *cnb1*Δ extracts, while phosphorylated peptides enriched in extracts of FK506-treated cells were largely distinct – perhaps due to differences between acute and chronic inactivation of CN (Figure 1B). This group of peptides represented many established CN substrates, including Crz1, Hph1, Rcn1, Slm1, and Aly1 (Figure 1B, Table S1) (Cyert and Philpott, 2013; O'Donnell et al., 2013). We used a second criterion to identify CN substrates more selectively by reasoning that most substrates would also contain a PxIxIT sequence. All previously characterized yeast substrates contain this docking motif, and a Cna1 mutant defective for PxIxIT binding fails to function *in vivo* (Roy et al., 2007). Therefore, we next determined which candidates also contained a putative PxIxIT site.

In silico identification of PxIxIT motifs

A consensus PxIxIT motif was derived by aligning 18 verified PxIxIT sites. The consensus excludes Pro and Gly, which may disrupt the extended conformation required for PxIxIT binding, from the degenerate 2^{nd} and 4^{th} positions, and accepts any hydrophilic residue in the sixth position (Figure 1C) (Bodmer et al., 2011; Minor and Kim, 1994; O'Donnell et al., 2013; Roy and Cyert, 2009). Like other SLiMs, PxIxIT sites must be surface accessible to mediate interaction with CN (Davey et al., 2012). Therefore, we identified PxIxIT sequences in the yeast proteome that were excluded from predicted globular and transmembrane domains, which distinguished many *bona fide* PxIxIT sites from other consensus matches (Table S2). Overall, 6% of yeast proteins (363/6000) contained one or more accessible PxIxIT sites (Table S2); however, 65 of 387 proteins with phosphorylated peptides that were more abundant in a CN-deficient extract contained these motifs (Figure 1D). This ~3-fold enrichment (17% vs. 6%) suggests that the presence of a PxIxIT motif has predictive power for identifying CN substrates. These 65 proteins, which include known CN substrates (Crz1, Aly1, Rcn1, Slm1) and interactors (Rcn2) (Mehta et al., 2009), were further analyzed.

Co-purification with CN in vivo

PxIxIT-mediated CN-substrate interactions are low-affinity. Therefore, to increase the sensitivity of our protein-interaction assay, GST fusions of each candidate substrate were expressed from a strong promoter in yeast that contained endogenously tagged catalytic subunit isoforms, Cna1 (Cna1-GFP) and Cna2 (Cna2-S-ZZ), and examined for co-purification with CN. Both isoforms co-purified with known CN substrates and interacting candidates but not with GST alone (Figure 2A). 33 of 42 candidates tested co-purified with one or both CNA isoforms (Figure 2A-B), 29 of which were newly identified as CN-interacting proteins (Table S3).

Direct dephosphorylation by CN in vitro identifies 15 new substrates

Finally, candidates were tested *in vitro* for their ability to be directly dephosphorylated by CN. Since phosphorylating kinases for these proteins were unknown, each protein was isolated from yeast extracts and hyperphosphorylated using co-purifying kinases prior to treatment with CN. 18 proteins, including established substrates, were significantly dephosphorylated by CN *in vitro* (Figure 3A) with many demonstrating a CN-dependent change in electrophoretic mobility (Figure 3B). However, the magnitude of dephosphorylation varied from 13-88%, reflecting differences either in the proportion of total phosphorylated residues that were susceptible to CN, and/or the extent to which CN-dependent sites on each substrate was dephosphorylated. Six proteins, including Rcn2, were not dephosphorylated by CN (non-substrates in Table S3), and nine others could not be tested due to insufficient incorporation of phosphate prior to incubation with CN (Table S3).

To confirm that PxIxIT docking was required for dephosphorylation of these new substrates, PVIVIT, a high affinity inhibitor of PxIxIT-mediated binding to CN, was included during dephosphorylation of a subset of candidates (Aramburu et al., 1999). Addition of this inhibitor attenuated CN-dependent dephosphorylation of Crz1, which has a verified PxIxIT site, as well as newly identified substrates Ubx7, Rod1, and Tda1 (Figure 3C-D, Figure S1) (Roy and Cyert, 2009). Thus, as predicted, these substrates require PxIxIT docking for dephosphorylation by CN.

These experiments identified 15 new CN substrates, more than doubling those identified previously (Figure 4A). The remaining novel CN-interacting proteins may represent regulators, scaffolds, or substrates that were not appropriately phosphorylated *in vitro* prior to their dephosphorylation (Figure 4A, Table S3 and references therein). Together, these 39 proteins establish the yeast CN signaling network, and represent the most comprehensive collection of CN-related signaling components yet identified.

Signaling network reveals new functions for CN

The CN signaling network is highly connected, (Figure S2) and enriched for several gene ontology categories, which surprisingly implicate CN in cell polarity – a function that has not been identified before (Figures 4A and 4B). Overall, this network augments our understanding of CN's established function in stress responses and suggests new regulatory roles for Ca^{2+}/CN signaling in polarized growth, autophagy, translation, ubiquitin signaling,

and Zn^{2+} homeostasis. We demonstrated the importance of protein regulation by CN in these processes by further characterizing the newly identified substrates Elm1 and Dig2.

CN inhibits Elm1 kinase activity

The Elm1 protein kinase regulates downstream kinases in several signaling pathways, but mechanisms governing its activity are unknown. Elm1 was hyperphosphorylated in CN-deficient cells as indicated by its reduced electrophoretic mobility, and deletion of the putative PxIxIT site ($Elm1^{\Delta PSIHID}$) abrogated CN-dependent dephosphorylation of Elm1 *in vivo* and *in vitro* (Figures 5A and 5B). Thus, Elm1 is regulated by CN in a PxIxIT-dependent manner.

To determine if Elm1 catalytic activity is regulated by CN, *in vitro* kinase assays were performed with Elm1 purified from *cnb1*Δ yeast in its phosphorylated or WT yeast in its dephosphorylated form. Phosphorylated Elm1 was significantly more active, and dephosphorylation by CN *in vitro* decreased the activity of both preparations to comparable levels (Figure 5E). We identified four sites in Elm1's C-terminal inhibitory domain (Sutherland et al., 2003) that were dephosphorylated by CN, by analyzing yeast extracts (S562, Table S1) and GST-Elm1 purified from CN-proficient or deficient cells (S516, S519, S581) (Figure 5C and Table S1). Substitution of Asp at these sites created Elm1-4D, a phosphomimetic mutant that showed decreased electrophoretic mobility and kinase activity that was resistant to CN (Figures 5D and 5E). These findings establish that CN negatively regulates Elm1 activity by dephosphorylating its C-terminal domain.

CN-dependent regulation of Elm1 *in vivo* was examined during alkaline stress, when yeast cells require Elm1-dependent activation of Snf1, the yeast AMP-activated kinase (AMPK), and CN-dependent activation of the Crz1 transcription factor (Casamayor et al., 2012). Snf1 and Crz1 co-regulate a set of genes, including *HXT2* and *ENA1* (Ruiz et al., 2008); thus, expression of these genes may be increased by CN via Crz1 and decreased by CN via inhibition of Elm1/Snf1. Indeed, under high pH conditions, *sak1*Δ *tos3*Δ *crz1*Δ cells, which lack Crz1 and depend solely on Elm1 to activate Snf1 (Sutherland et al., 2003), showed increased expression of *HXT2-lacZ* when CN was inhibited with FK506 (Figure 5F); similar results were obtained for *ENA1-lacZ* (data not shown). In contrast, during glucose starvation, which activates Snf1 but not CN, expression of *HXT2-lacZ* was unaltered by FK506 (Figure S3A). Thus, CN inhibits Elm1 during alkaline stress (Figure 5H). Although this repression seems paradoxical for genes that are also induced by CN/ Crz1, published data shows that 52 Crz1-independent genes are repressed by CN during alkaline stress; thus, attenuation of gene expression by CN is a distinct feature of this response (Table S4) (Viladevall et al., 2004). Furthermore, repression of this pathway by CN may be conserved; in rat hippocampus, CN inhibitors activate LKB1 and TAK1, AMPK-activating kinases that have sequence similarity to Elm1 (Park et al., 2011).

We further examined CN-dependent regulation of Elm1 during progression through the G_1 phase of the cell cycle. *elm1*Δ is lethal when combined with deletions of the redundant G_1 cyclins, and as expected, the growth rate of a *cln1*Δ *cln2*Δ strain expressing an analog-sensitive allele (*elm1-as*) was reduced in the presence of low amounts of the 1-NM-PP1inhibitor (Figure 5G) (Sreenivasan et al., 2003). Growth of this strain significantly

improved upon inhibition of CN with FK506, consistent with an increase in Elm1 activity (Figure 5G). Neither 1-NM-PP1 nor FK506 treatment altered the growth rate of a wild type or *cln1*Δ *cln2*Δ strain, or *CLN1 CLN2* cells expressing Elm1-as (Figure S3B, data not shown). Thus, CN inhibits progression through G1 via Elm1 and may contribute to growth attenuation during stress (Figure 5I). CN may similarly restrict other cell cycle processes that depend on Elm1, including septin organization and cytokinesis (Asano et al., 2006), the G_2/M morphogenesis checkpoint (Szkotnicki et al., 2008), and the spindle position checkpoint (Moore et al., 2010).

CN negatively regulates pheromone signaling via Dig2

The identification of Dig2 as a CN substrate provides a possible mechanism for CN-dependent inhibition of the yeast mating response (reviewed in (Cyert and Philpott, 2013). Dig2 and its paralog, Dig1, form an inhibitory complex with the Ste12 transcriptional activator (Bardwell, 2005). Upon pheromone addition, the Fus3 MAPK phosphorylates Dig1 and Dig2 to relieve this inhibition, and directly phosphorylates and activates Ste12.

To investigate the regulation of Dig2 by CN, we first demonstrated that yeast CN co-purified with the predicted PxIxIT sequence in Dig2 (GST-Dig2$^{95\text{-}116}$) and that mutation of critical residues decreased this binding (GST-Dig2$^{95\text{-}116,\ Mut}$) (Figures 6A and 6D). *In vivo*, pheromone-induced expression of *FUS1-lacZ*, a Ste12-dependent transcriptional reporter, was significantly higher in *dig1*Δ cells that expressed Dig2^{Mut} rather than Dig2 (Figure 6B). Furthermore, in the presence or absence of pheromone, expression of low levels of constitutively active CN (CN*) significantly reduced *FUS1-lacZ* activity in Dig2-expressing cells, but not in Dig2^{Mut} cells. (Figures 6B and S4). This effect required CN catalytic activity, and was abrogated by FK506 or expression of CN*mut that was catalytically inactive (Figures 6B and S4). Consistent with its effect on Dig2 function, CN* decreased the phosphorylation of GST-Dig2, but not GST-Dig2^{Mut} (Figure 6C). Thus, CN negatively regulates Ste12-mediated transcription *in vivo* by dephosphorylating Dig2, and this inhibition is disrupted in Dig2^{Mut}.

Surprisingly, the overall phosphorylation of GST-Dig2^{Mut} was decreased relative to GST-Dig2 (Figure 6C), which was unexpected given its reduced interaction with CN. We discovered that the Dig2 PxIxIT sequence overlaps with a previously identified MAPK docking site, or D-site, which binds to both Fus3 and Kss1 MAPKs (Kusari et al., 2004) (Figure 6D). D-sites contain a cluster of basic residues located 3-5 residues upstream of two hydrophobic residues, and an overlapping PxIxIT/D-site is formed when these hydrophobic residues contribute to both motifs. Therefore, GST-Dig2^{Mut} was tested for decreased interaction with Fus3. GST-Dig2$^{95\text{-}116}$ but not GST-Dig2$^{95\text{-}116,\ Mut}$ co-purified with Fus3 *in vitro* and CN directly competed with Fus3 for binding to GSTDig2$^{95\text{-}116}$ (Figures 6D and 6E). Thus, the increased signaling mediated by Dig2^{Mut} *in vivo* is the result of reduced interactions with both CN and Fus3, which may act on different sets of phosphorylation sites. Together, our findings show that CN inhibits the pheromone response both by dephosphorylating Dig2 and by displacing Fus3 (Figure 6F). This competition may contribute to switch-like behavior during pheromone response, as was shown for

competitive binding between Fus3 and the Ptc1 phosphatase to Ste5, a scaffold that organizes mating pathway kinases (Malleshaiah et al., 2010).

Moreover, overlapping PxIxIT/D-sites were broadly identified. CN network components, Aly1 and Kic1, were among the yeast proteins predicted to contain such motifs (Table S2). In mammals, a PxIxIT consensus match overlapped a verified D-site in the JunB transcription factor, which binds to JNK family MAPKs (Whisenant et al., 2010). We demonstrated that human CN did co-purify with this region, GST-JunB$^{31\text{-}48}$, *in vitro* and that mutation of the predicted PxIxIT site decreased binding (GST-JunB$^{31\text{-}48\ Mut}$, Figures 6G and 6H). Therefore, CN and JNK likely compete for JunB *in vivo*, and multiple examples of such composite PxIxIT/D-sites occur in a set of predicted JNK-binding D-sites (Table S5) (Whisenant et al., 2010). Our study is thus the first to demonstrate direct competition between CN and MAPKs for substrates and establish a new regulatory feature of eukaryotic signaling pathways.

The majority of PxIxIT sites in the CN signaling network evolved recently

Next, we considered how CN signaling networks evolve and examined a role for PxIxIT sites in determining network identity. Using protein alignments of fungal species that span 600 million years of divergence, we examined the conservation of predicted PxIxIT consensus matches in CN network proteins relative to control scrambled PxIxIT sequences in the same protein (Figures 7A and S5B) (Wapinski et al., 2007). The conservation of PxIxIT matches that were located in inaccessible protein domains, thus judged to be non-functional, was strongly correlated with that of scrambled sequences, suggesting that they evolve under similar constraints (Figure S5B). Functional motifs, i.e. those demonstrated to bind CN, or located within accessible protein domains, included some that were broadly conserved (Rcn1, Rcn2, Crz1) but others that showed no evidence of increased conservation relative to scrambled sequences (Elm1, Aly1, Dig2) (Figure 7A). In fact, 70% of PxIxIT motifs in CN network proteins were found only within the *Saccharomyces sensu stricto* clade, which radiated from a common ancestor ~20 million years ago (Figures 7B and S5A) (Wapinski et al., 2007). Thus, these relatively young sites either reflect rapid turnover of PxIxIT sequences via neutral gains and losses, or were fixed only recently by natural selection.

To demonstrate that acquisition of a PxIxIT site during evolution confers CN-dependent regulation, we expressed Elm1 orthologs from the *sensu stricto* species in *S. cerevisiae*. Each ortholog was more than 75% identical to *S. cerevisiae* Elm1 and contained at least 3 of 4 CN-dependent phosphorylation sites. Elm1 from *S. paradoxus*, but not *S. mikatae* or *S. bayanus*, was predicted to contain a functional PxIxIT motif (Figure 7C). Consistent with this prediction, both *S. cerevisiae* and *S. paradoxus* Elm1 displayed reduced electrophoretic mobility in cells treated with the CN inhibitor, FK506, and all phosphorylated forms of these proteins collapsed to a single fast-migrating band upon incubation with λ phosphatase (Figure 7D). In contrast, *S. mikatae* and *S. bayanus* Elm1 displayed no FK506-dependent change in electrophoretic mobility, but did migrate faster after dephosphorylation with λ phosphatase (Figure 7D), indicating that, although phosphorylated, their phosphorylation status was not regulated by CN. These data strongly suggest that Elm1 joined the CN

signaling network recently through its acquisition of a PxIxIT site. Similarly, analyses of Tda1 homologs from *S. paradoxus* and *S. mikatae*, which contain PxIxIT matches, and *S. bayanus*, which does not (Figure S5C), suggested that CN regulated the phosphorylation status of all but *S. bayanus* Tda1 (Figure S5D). In contrast, all *sensu stricto* Crz1 homologs contained a conserved PxIxIT site and displayed a CN-dependent shift in electrophoretic mobility (Figure S5E).

To test directly if acquisition of a PxIxIT sequence could recruit a new protein to the CN signaling network, we modified *S. mikatae* Elm1 to introduce the PxIxIT sequence from its *S. cerevisiae* homolog (VSSHTD changed to PSIHID, Figure 7C). In contrast to *S. mikatae* Elm1, *S. mikatae* Elm1^{PSIHID} was dephosphorylated by CN *in vitro*, resulting in increased electrophoretic mobility (Figure 7E). As expected, the ability of CN to dephosphorylate *S. cerevisiae* Elm1 *in vitro* was abrogated when the PxIxIT sequence was deleted (Elm1$^{\Delta PSIHID}$, Figures 7E, 5A and 5B). Together, these analyses indicate that PxIxIT motifs are a primary determinant of CN network identity, and that their gains and losses drive evolution of the network.

The predominance of recently acquired PxIxIT sites in the yeast CN network predicts poor conservation of CN-regulated proteins over long evolutionary time, i.e. between yeast and mammals, which diverged ~1.2 billion years ago. We identified 37 high confidence mammalian CN substrates from the literature (Table S7) (Li et al., 2013) and found that only RCAN1 and Synaptojanin-1 were homologous to yeast CN network proteins (Figures 7F and 7G). This rewiring of the CN signaling network may be facilitated by rapid change in phosphorylation sites, many of which localize to disordered regions (Levy et al., 2012), and in PxIxIT motifs, which confer CN-dependent regulation. This mode of rewiring is reminiscent of other networks that rely on SLiMs, such as SH3 interaction networks that are driven by rapid change in SH3 binding sites (Sun et al., 2012).

Similar kinase families phosphorylate divergent CN substrates in yeast and mammals

Our results with MAPKs suggest that kinases and phosphatases are functionally coupled through recognition of common binding sites in their substrates. Thus, although the targets of phosphorylation networks turnover rapidly, particular kinase-phosphatase pairs may persist as conserved network motifs. Consistent with this model, we noted that CN opposes PKA signaling in both yeast and mammals, despite extensive divergence in targets (Cyert and Roy, 2013). In yeast, antagonistic CN-PKA signaling corresponds to the opposing processes they regulate, i.e. stress responses vs. growth (Kafadar and Cyert, 2004), and in this study, we noted that phosphorylated peptides containing PKA consensus motifs were significantly enriched in CN-deficient yeast extracts (Figure S1B).

Therefore, we used bioinformatic tools and high-confidence interaction data to identify protein kinases that were associated with yeast and mammalian CN substrates. The yeast CN signaling network was significantly enriched for substrates of 21 distinct protein kinase families ($p \leq 0.03$, see supplemental methods) (Figure 7F, Table S5) (Sharifpoor et al., 2011), which included cyclin-dependent kinases (CDKs) in addition to PKA and MAPK, consistent with the alleviating genetic interaction observed between and *cdc28*-DAmP (Fiedler et al., 2009). Substrates of 15 kinase families were significantly overrepresented

among mammalian CN targets ($p \leq 0.03$) (Figure 7G, Table S6) (Lachmann and Ma'ayan, 2009). Most importantly, the kinases associated with CN-regulated proteins in yeast and mammals were highly similar, with 9 kinase families strongly associating with both networks ($p \leq 2.8\times10^{-5}$) (Figures 7F and 7G, Tables S5 and S6). These include both basophilic (PKA, PKC, AKT, CAMKL) and proline-directed (GSK3, CDK, MAPK) kinases (Hanks and Hunter, 1995). Thus, during network evolution, the conservation of CN-kinase regulatory modules transcends rapid turnover in substrates.

We propose that conserved structural features of targets maintain CN-kinase opposition during evolution. CN and particular kinases recognize similar phosphorylation motifs: CN tolerates Pro in the +1 position, which defines the specificity of proline-directed kinases, and slightly favors sites with a basic residue in the -3 position, a motif recognized by basophilic kinases (Dinkel et al., 2012; Donella-Deana et al., 1994; Grigoriu et al., 2013; Li et al., 2013). However, the broad range of sequences acted upon by CN and other phosphatases suggests that simple recognition of phosphorylation motifs is insufficient to preserve kinase-phosphatase opposition in networks (Li et al., 2013). Significantly, like phosphatases, many kinases rely on docking sequences to recognize their substrates, and, as we show here for CN and MAPK, recognition of similar docking sequences by a kinase and phosphatase reinforces substrate co-regulation. Other examples of such overlapping docking sites have been described, and will likely emerge as a common feature of phosphorylation networks (Bhaduri and Pryciak, 2011; Hirschi et al., 2010). Together, both factors reinforce the identity of kinase-phosphatase modules in evolving networks.

Significance

Phosphorylation-based signaling networks regulate the vast majority of cellular processes and evolve to acquire new regulatory outputs. Many factors, including the modularity of protein interactions, contribute to evolvability (Bhattacharyya et al., 2006). Our findings reveal a new design principle of phosphorylation networks, namely the functional coupling of a kinase and phosphatase, which preserves network architecture as regulatory targets change. Such higher-order conservation has been reported for other types of networks: during evolution of transcriptional networks, the DNA binding specificity of regulators is conserved, but the gene sets they modulate may diverge (Li and Johnson, 2010). Alternatively, groups of genes may maintain their co-regulation during evolution while the identity of their transcriptional regulator changes (Tanay et al., 2005). Kinase-phosphatase linkage offers several advantages for network rewiring. First, the ability of targets to acquire co-regulation by a kinase and phosphatase would mitigate possible negative consequences of unopposed phosphorylation sites; this argument has also been applied to the evolution of phosphotyrosine signaling, where the emergence of protein tyrosine phosphatases preceded the expansion of tyrosine kinases (Lim and Pawson, 2010). Second, studies of transcriptional networks show that evolution of secondary regulatory features, such as feed forward loops, is favored when two regulators share a common target (Ward and Thornton, 2007). There are multiple examples of such motifs in CN signaling networks. Mammalian CN dephosphorylates CK1ε, GSK3β, and the RII regulatory subunit of PKA, which in turn, phosphorylate CN substrates (Table S6). Furthermore, the scaffold protein AKAP79/150 co-localizes CN and PKA with key substrates (Welch et al., 2010).

Our study demonstrates that systematic identification of phosphatase substrates is feasible and critical to understand signaling networks. Modeling of kinase signaling has already yielded insights into disease and sponsored new therapeutic treatments (Logue and Morrison, 2012). However, information about phosphatases has lagged behind. Combinatorial therapies, which require lower drug levels and reduce harmful side effects, may be possible once both the kinase and phosphatase regulators of critical disease proteins are known. CN inhibitors are currently widely prescribed but are also associated with toxicities that result from reduction of CN activity in multiple tissues (Safa et al., 2013). Furthermore, perturbation in CN signaling is associated with a broad spectrum of disorders, including neurodegenerative diseases, cardiac hypertrophy, cancer, and diabetes (Cyert and Roy, 2013). Thorough elucidation of CN signaling networks not only provides new insights into the functions of this regulator but may also unveil new strategies to selectively modulate its targets.

Experimental Procedures

Growth media and general methods

S. cerevisiae strains were grown in YPD or synthetic complete (SC) media and transformed as previously described (Roy et al., 2007). Where noted, FK506 (LC Laboratories, Woburn, MA) was used at 1 μg/mL (from a 10 mg/mL stock in ET buffer -90% ethanol, 10% Tween-20), 1-NM-PP1 (Cayman Chemical, Ann Arbor, MI) was used at 1 μM (from a 250 μM stock in DMSO), $CaCl_2$ (Sigma-Aldrich, St. Louis, MO) was used at 200 mM (from a 3M stock in water), andα-factor (GenScript, Piscataway, NJ) was used at 1-2 μg/mL.

Yeast strains and plasmids

Yeast strains and plasmids used in this study are listed in Tables S7 and S8. See supplemental experimental procedures for details of strain origin and construction.

Analysis of the CN-dependent phosphoproteome by mass spectrometry

Growth conditions, sample preparation, label-free LC-MS/MS measurements, and downstream bioinformatics analysis of detected peptides were carried out as described previously (Bodenmiller et al., 2010) except for modifications detailed in the supplement. For all preparations, $CaCl_2$ was added 10 minutes prior to cell harvesting to activate CN. Criteria for designating phosphorylated peptides as CN-dependent are detailed in the supplement.

Identification of putative docking motifs in silico

Verified PxIxIT motifs were aligned using WebLogo (Crooks et al., 2004). Biopython (Cock et al., 2009) was used to query the PxIxIT consensus (P[^PG][IVLF][^PG][IVLF][TSHEDQNKR]) against S288C ORF translations (Cherry et al., 2012). Globular domain prediction was performed using GlobPlot with default web settings (Linding et al., 2003). Transmembrane domain prediction was performed using HMMTOP with default settings (Tusnady and Simon, 2001).

Co-purification assays

JRY11 cells expressing GST-tagged proteins were grown in SC −URA 2% Raf at 30°C to OD_{600} 0.6-0.8, induced with 2% Gal for 4 hours, treated with $CaCl_2$ for 10 minutes prior to harvesting, and extracted by glass bead lysis in low salt RIPA buffer. GST-tagged proteins were purified using glutathione-Sepharose beads from 5 mg of protein extract for normal expressors, or 12-17 mg for low expressors, and subjected to immunoblot analysis. Methods are further detailed in the supplement.

In vitro phosphatase assay

GST-tagged ORFs (expressed in BY4741::*cnb1*Δ, no $CaCl_2$ addition) were purified from 2-25 mg of extract as described above, washed 2X in low salt RIPA, 1X in kinase buffer (KB: 50 mM Tris-HCl pH 7.5, 10 mM $MgCl_2$, 1 mM DTT), resuspended in KB supplemented with 1 mM ATP (pH 7.5) and 1 μL ATP, [γ-^{32}P] (3000 Ci/mmol) (Perkin Elmer Cetus), incubated at 32°C for 30 min, and washed 3X with KB to remove unincorporated ATP. For Figures 3A and 5E, each sample was split and incubated at 32°C for 45 min with either no CN (mock) or 0.5 μg recombinant, constitutively active, yeast CN (purified as described in supplement). For Figure 3C, samples were divided into three parts and incubated with KB containing no CN, 0.5 μg CN, or 0.5 μg CN with 200 μM PVIVIT (GPHPVIVITGPHEE) peptide (Aramburu et al., 1999). Samples were analyzed using SDS-PAGE and Gelcode Blue (GE Life Sciences, Little Chalfont, Buckinghamshire, United Kingdom). ^{32}P content was quantified using a Typhoon Scanner (GE Healthcare) and normalized to protein level, as determined by ImageJ analysis of stained protein bands (Schneider et al., 2012).

Supplementary Material

Refer to Web version on PubMed Central for supplementary material.

Acknowledgments

We thank Drs. D. Kellogg, S. Michnick, P. Pryciak, and M. Schmidt for reagents, Drs. J. Skotheim and A. Kaushal for helpful discussion, and Drs. J. Taggart and D. Eide for sharing unpublished data. We thank M. Conlon and P. Picotti for technical assistance and R. Bond, E. Guiney, and N. Ly for reagents and critical reading of the manuscript. M.S.C. and J.R. are supported by NIH grant GM-48728. A.G. was supported by T32-GM007276 and GM-48728. B.B. was supported by fellowships of the Swiss National Science Foundation (SNF), the European Molecular Biology Organization (EMBO), and the Marie Curie IOF. C.R.L. is supported by Canadian Institute of Health Research (CIHR) grant GMX-191597.

References

Aramburu J, Garcia-Cozar F, Raghavan A, Okamura H, Rao A, Hogan PG. Selective inhibition of NFAT activation by a peptide spanning the calcineurin targeting site of NFAT. Mol Cell. 1998; 1:627–637. [PubMed: 9660947]

Aramburu J, Yaffe MB, Lopez-Rodriguez C, Cantley LC, Hogan PG, Rao A. Affinity-driven peptide selection of an NFAT inhibitor more selective than cyclosporin A. Science. 1999; 285:2129–2133. [PubMed: 10497131]

Asano S, Park JE, Yu LR, Zhou M, Sakchaisri K, Park CJ, Kang YH, Thorner J, Veenstra TD, Lee KS. Direct phosphorylation and activation of a Nim1-related kinase Gin4 by Elm1 in budding yeast. J Biol Chem. 2006; 281:27090–27098. [PubMed: 16861226]

Bardwell L. A walk-through of the yeast mating pheromone response pathway. Peptides. 2005; 26:339–350. [PubMed: 15690603]

Bhaduri S, Pryciak PM. Cyclin-specific docking motifs promote phosphorylation of yeast signaling proteins by G1/S Cdk complexes. Curr Biol. 2011; 21:1615–1623. [PubMed: 21945277]

Bhattacharyya RP, Remenyi A, Yeh BJ, Lim WA. Domains, motifs, and scaffolds: the role of modular interactions in the evolution and wiring of cell signaling circuits. Annual review of biochemistry. 2006; 75:655–680.

Bodenmiller B, Wanka S, Kraft C, Urban J, Campbell D, Pedrioli PG, Gerrits B, Picotti P, Lam H, Vitek O, et al. Phosphoproteomic analysis reveals interconnected system-wide responses to perturbations of kinases and phosphatases in yeast. Sci Signal. 2010; 3:rs4. [PubMed: 21177495]

Bodmer D, Ascano M, Kuruvilla R. Isoform-specific dephosphorylation of dynamin1 by calcineurin couples neurotrophin receptor endocytosis to axonal growth. Neuron. 2011; 70:1085–1099. [PubMed: 21689596]

Breitkreutz A, Choi H, Sharom JR, Boucher L, Neduva V, Larsen B, Lin ZY, Breitkreutz BJ, Stark C, Liu G, et al. A global protein kinase and phosphatase interaction network in yeast. Science. 2010; 328:1043–1046. [PubMed: 20489023]

Casamayor A, Serrano R, Platara M, Casado C, Ruiz A, Arino J. The role of the Snf1 kinase in the adaptive response of Saccharomyces cerevisiae to alkaline pH stress. Biochem J. 2012; 444:39–49. [PubMed: 22372618]

Cherry JM, Hong EL, Amundsen C, Balakrishnan R, Binkley G, Chan ET, Christie KR, Costanzo MC, Dwight SS, Engel SR, et al. Saccharomyces Genome Database: the genomics resource of budding yeast. Nucleic Acids Res. 2012; 40:D700–705. [PubMed: 22110037]

Cock PJ, Antao T, Chang JT, Chapman BA, Cox CJ, Dalke A, Friedberg I, Hamelryck T, Kauff F, Wilczynski B, et al. Biopython: freely available Python tools for computational molecular biology and bioinformatics. Bioinformatics. 2009; 25:1422–1423. [PubMed: 19304878]

Crooks GE, Hon G, Chandonia JM, Brenner SE. WebLogo: a sequence logo generator. Genome Res. 2004; 14:1188–1190. [PubMed: 15173120]

Cyert MS, Philpott CC. Regulation of Cation Balance in Saccharomyces cerevisiae. Genetics. 2013; 193:677–713. [PubMed: 23463800]

Cyert, MS.; Roy, J. Encyclopedia of Metalloproteins, U.V.N. Kretsinger, RH.; Permyakov, EA., editors. Springer; New York: 2013. p. 392-402.

Davey NE, Van Roey K, Weatheritt RJ, Toedt G, Uyar B, Altenberg B, Budd A, Diella F, Dinkel H, Gibson TJ. Attributes of short linear motifs. Molecular bioSystems. 2012; 8:268–281. [PubMed: 21909575]

Dinkel H, Michael S, Weatheritt RJ, Davey NE, Van Roey K, Altenberg B, Toedt G, Uyar B, Seiler M, Budd A, et al. ELM--the database of eukaryotic linear motifs. Nucleic Acids Res. 2012; 40:D242–251. [PubMed: 22110040]

Donella-Deana A, Krinks MH, Ruzzene M, Klee C, Pinna LA. Dephosphorylation of phosphopeptides by calcineurin (protein phosphatase 2B). European journal of biochemistry / FEBS. 1994; 219:109–117. [PubMed: 7508382]

Fiedler D, Braberg H, Mehta M, Chechik G, Cagney G, Mukherjee P, Silva AC, Shales M, Collins SR, van Wageningen S, et al. Functional organization of the S. cerevisiae phosphorylation network. Cell. 2009; 136:952–963. [PubMed: 19269370]

Grigoriu S, Bond R, Cossio P, Chen JA, Ly N, Hummer G, Page R, Cyert MS, Peti W. The molecular mechanism of substrate engagement and immunosuppressant inhibition of calcineurin. PLoS biology. 2013; 11:e1001492. [PubMed: 23468591]

Hanks SK, Hunter T. Protein kinases 6. The eukaryotic protein kinase superfamily: kinase (catalytic) domain structure and classification. FASEB journal : official publication of the Federation of American Societies for Experimental Biology. 1995; 9:576–596. [PubMed: 7768349]

Hendrickx A, Beullens M, Ceulemans H, Den Abt T, Van Eynde A, Nicolaescu E, Lesage B, Bollen M. Docking motif-guided mapping of the interactome of protein phosphatase-1. Chem Biol. 2009; 16:365–371. [PubMed: 19389623]

Hirschi A, Cecchini M, Steinhardt RC, Schamber MR, Dick FA, Rubin SM. An overlapping kinase and phosphatase docking site regulates activity of the retinoblastoma protein. Nat Struct Mol Biol. 2010; 17:1051–1057. [PubMed: 20694007]

Kafadar KA, Cyert MS. Integration of stress responses: modulation of calcineurin signaling in Saccharomyces cerevisiae by protein kinase A. Eukaryot Cell. 2004; 3:1147–1153. [PubMed: 15470242]

Kingsbury TJ, Cunningham KW. A conserved family of calcineurin regulators. Genes Dev. 2000; 14:1595–1604. [PubMed: 10887154]

Kusari AB, Molina DM, Sabbagh W Jr. Lau CS, Bardwell L. A conserved protein interaction network involving the yeast MAP kinases Fus3 and Kss1. J Cell Biol. 2004; 164:267–277. [PubMed: 14734536]

Lachmann A, Ma'ayan A. KEA: kinase enrichment analysis. Bioinformatics. 2009; 25:684–686. [PubMed: 19176546]

Levy ED, Michnick SW, Landry CR. Protein abundance is key to distinguish promiscuous from functional phosphorylation based on evolutionary information. Philosophical transactions of the Royal Society of London Series B, Biological sciences. 2012; 367:2594–2606.

Li H, Johnson AD. Evolution of transcription networks--lessons from yeasts. Curr Biol. 2010; 20:R746–753. [PubMed: 20833319]

Li H, Zhang L, Rao A, Harrison SC, Hogan PG. Structure of calcineurin in complex with PVIVIT peptide: portrait of a low-affinity signalling interaction. J Mol Biol. 2007; 369:1296–1306. [PubMed: 17498738]

Li X, Wilmanns M, Thornton J, Kohn M. Elucidating Human Phosphatase-Substrate Networks. Sci Signal. 2013; 6:rs10. [PubMed: 23674824]

Lim WA, Pawson T. Phosphotyrosine signaling: evolving a new cellular communication system. Cell. 2010; 142:661–667. [PubMed: 20813250]

Linding R, Russell RB, Neduva V, Gibson TJ. GlobPlot: Exploring protein sequences for globularity and disorder. Nucleic Acids Res. 2003; 31:3701–3708. [PubMed: 12824398]

Logue JS, Morrison DK. Complexity in the signaling network: insights from the use of targeted inhibitors in cancer therapy. Genes Dev. 2012; 26:641–650. [PubMed: 22474259]

Malleshaiah MK, Shahrezaei V, Swain PS, Michnick SW. The scaffold protein Ste5 directly controls a switch-like mating decision in yeast. Nature. 2010; 465:101–105. [PubMed: 20400943]

Mehta S, Li H, Hogan PG, Cunningham KW. Domain architecture of the regulators of calcineurin (RCANs) and identification of a divergent RCAN in yeast. Mol Cell Biol. 2009; 29:2777–2793. [PubMed: 19273587]

Minor DL Jr. Kim PS. Measurement of the beta-sheet-forming propensities of amino acids. Nature. 1994; 367:660–663. [PubMed: 8107853]

Moore JK, Chudalayandi P, Heil-Chapdelaine RA, Cooper JA. The spindle position checkpoint is coordinated by the Elm1 kinase. J Cell Biol. 2010; 191:493–503. [PubMed: 21041444]

Moses AM, Landry CR. Moving from transcriptional to phospho-evolution: generalizing regulatory evolution? Trends Genet. 2010; 26:462–467. [PubMed: 20817339]

O'Donnell AF, Huang L, Thorner J, Cyert MS. A calcineurin-dependent switch controls the trafficking function of alpha-arrestin Aly1/Art6. J Biol Chem. 2013; 288:24063–24080. [PubMed: 23824189]

Park HG, Yi H, Kim SH, Yu HS, Ahn YM, Lee YH, Roh MS, Kim YS. The effect of cyclosporine A on the phosphorylation of the AMPK pathway in the rat hippocampus. Progress in neuro-psychopharmacology & biological psychiatry. 2011; 35:1933–1937. [PubMed: 21963396]

Rodriguez A, Roy J, Martinez-Martinez S, Lopez-Maderuelo MD, Nino-Moreno P, Orti L, Pantoja-Uceda D, Pineda-Lucena A, Cyert MS, Redondo JM. A conserved docking surface on calcineurin mediates interaction with substrates and immunosuppressants. Mol Cell. 2009; 33:616–626. [PubMed: 19285944]

Roux PP, Thibault P. The coming of age of phosphoproteomics; from large data sets to inference of protein functions. Mol Cell Proteomics. 2013

Roy J, Cyert MS. Cracking the phosphatase code: docking interactions determine substrate specificity. Sci Signal. 2009; 2:re9. [PubMed: 19996458]

Roy J, Li H, Hogan PG, Cyert MS. A conserved docking site modulates substrate affinity for calcineurin, signaling output, and in vivo function. Mol Cell. 2007; 25:889–901. [PubMed: 17386265]

Ruiz A, Serrano R, Arino J. Direct regulation of genes involved in glucose utilization by the calcium/calcineurin pathway. J Biol Chem. 2008; 283:13923–13933. [PubMed: 18362157]

Safa K, Riella LV, Chandraker A. Beyond calcineurin inhibitors: emerging agents in kidney transplantation. Current opinion in nephrology and hypertension. 2013

Schneider CA, Rasband WS, Eliceiri KW. NIH Image to ImageJ: 25 years of image analysis. Nat Methods. 2012; 9:671–675. [PubMed: 22930834]

Sharifpoor S, Nguyen Ba AN, Young JY, van Dyk D, Friesen H, Douglas AC, Kurat CF, Chong YT, Founk K, Moses AM, et al. A quantitative literature-curated gold standard for kinase-substrate pairs. Genome Biol. 2011; 12:R39. [PubMed: 21492431]

Sreenivasan A, Bishop AC, Shokat KM, Kellogg DR. Specific inhibition of Elm1 kinase activity reveals functions required for early G1 events. Mol Cell Biol. 2003; 23:6327–6337. [PubMed: 12917352]

Steinbach WJ, Reedy JL, Cramer RA Jr. Perfect JR, Heitman J. Harnessing calcineurin as a novel anti-infective agent against invasive fungal infections. Nature reviews Microbiology. 2007; 5:418–430.

Sun MG, Sikora M, Costanzo M, Boone C, Kim PM. Network evolution: rewiring and signatures of conservation in signaling. PLoS computational biology. 2012; 8:e1002411. [PubMed: 22438796]

Sutherland CM, Hawley SA, McCartney RR, Leech A, Stark MJ, Schmidt MC, Hardie DG. Elm1p is one of three upstream kinases for the Saccharomyces cerevisiae SNF1 complex. Curr Biol. 2003; 13:1299–1305. [PubMed: 12906789]

Szkotnicki L, Crutchley JM, Zyla TR, Bardes ES, Lew DJ. The checkpoint kinase Hsl1p is activated by Elm1p-dependent phosphorylation. Mol Biol Cell. 2008; 19:4675–4686. [PubMed: 18768748]

Tanay A, Regev A, Shamir R. Conservation and evolvability in regulatory networks: the evolution of ribosomal regulation in yeast. Proc Natl Acad Sci U S A. 2005; 102:7203–7208. [PubMed: 15883364]

Tusnady GE, Simon I. The HMMTOP transmembrane topology prediction server. Bioinformatics. 2001; 17:849–850. [PubMed: 11590105]

Viladevall L, Serrano R, Ruiz A, Domenech G, Giraldo J, Barcelo A, Arino J. Characterization of the calcium-mediated response to alkaline stress in Saccharomyces cerevisiae. J Biol Chem. 2004; 279:43614–43624. [PubMed: 15299026]

Wapinski I, Pfeffer A, Friedman N, Regev A. Natural history and evolutionary principles of gene duplication in fungi. Nature. 2007; 449:54–61. [PubMed: 17805289]

Ward JJ, Thornton JM. Evolutionary models for formation of network motifs and modularity in the Saccharomyces transcription factor network. PLoS computational biology. 2007; 3:1993–2002. [PubMed: 17967049]

Welch EJ, Jones BW, Scott JD. Networking with AKAPs: context-dependent regulation of anchored enzymes. Molecular interventions. 2010; 10:86–97. [PubMed: 20368369]

Whisenant TC, Ho DT, Benz RW, Rogers JS, Kaake RM, Gordon EA, Huang L, Baldi P, Bardwell L. Computational prediction and experimental verification of new MAP kinase docking sites and substrates including Gli transcription factors. PLoS computational biology. 2010; 6

Won AP, Garbarino JE, Lim WA. Recruitment interactions can override catalytic interactions in determining the functional identity of a protein kinase. Proc Natl Acad Sci U S A. 2011; 108:9809–9814. [PubMed: 21628578]

Highlights

- First systematic identification of substrates for a phosphatase
- Calcineurin network rewiring is mediated by docking site gain and loss
- Select docking sites confer dual regulation by a kinase and phosphatase
- Calcineurin substrates diverge but are phosphorylated by a conserved group of kinases

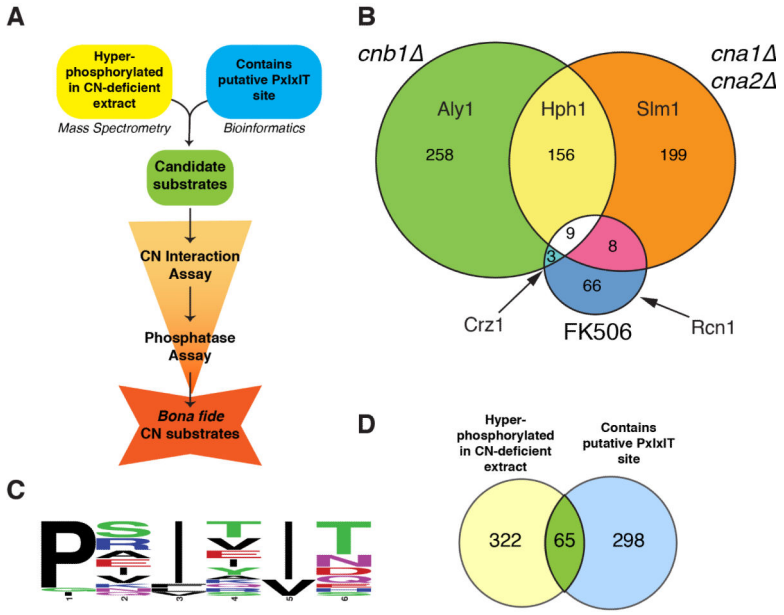

Figure 1. Characterization of the CN-dependent phosphoproteome

(A) Strategy used to identify CN substrates. (B) Overlap between the 699 phosphorylated peptides enriched in CN-deficient samples identified in distinct screens. Phosphorylated peptides from verified CN substrates are labeled. See also Figure S1A,C and Table S1. (C) Logo of 18 verified PxIxIT motifs used to generate the consensus motif: P[^PG][IVLF][^PG][IVLF][TSHEDQNKR]. See also Figure S1B and Table S2. (D) Overlap between 363 proteins with a predicted accessible PxIxIT motif and 387 proteins with one or more calcineurin-regulated phosphorylated peptide. See also Table S3.

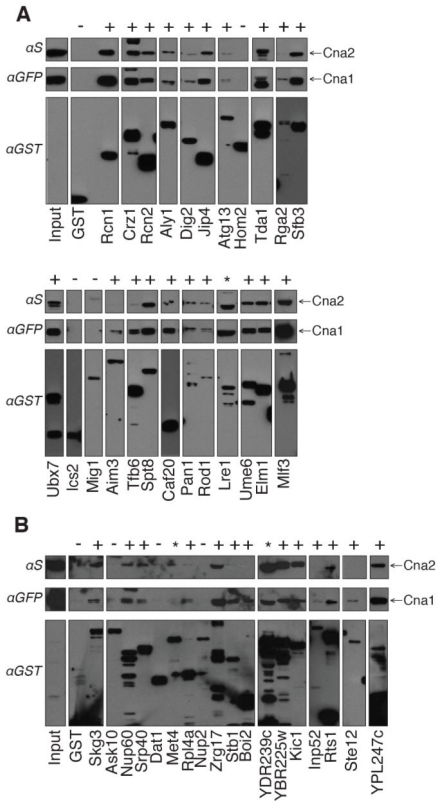

Figure 2. Interaction of candidates with CN

(A) High- or (B) low-expressing GST-candidate fusions were purified from strain JRY11 to assay co-purification with Cna2-STEV-ZZ (αS) and Cna1-GFP (αGFP). Candidates classified as interactors (+), noninteractors (-), or ambiguous (*). See also Table S3.

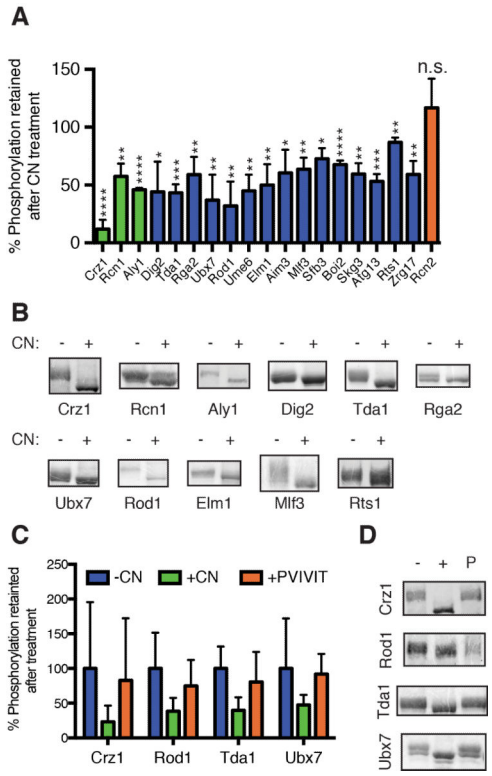

Figure 3. Identification of new CN substrates

(A) *In vitro* dephosphorylation of GST candidate fusions by CN. "% Phosphorylation retained after CN treatment": Normalized ^{32}P content of each CN-treated sample was compared to its paired mock-treated sample, which was set to 100%; for each protein, experimental replicates were averaged. Established (green) and new (blue) substrates and non-substrates (red) are shown (n = 2 for Aly1, Rcn1, and Atg13, n ≥ 3 for all others). Error bars represent 1 SD. Data were analyzed by Student's T-test. * $p < 0.05$, ** $p < 0.01$, *** $p < 0.001$, and **** $p < 0.0001$. See also Table S3. (B) Substrates that showed electrophoretic mobility changes in CN-treated (+) vs. mock-treated (-) samples. (C) Dephosphorylation of Crz1, Rod1, Tda1 and Ubx7 is inhibited by high-affinity PVIVIT peptide. "% Phosphorylation retained after treatment": Normalized ^{32}P contents of mock-treated, CN-treated, and CN + PVIVIT-treated samples were determined for each experimental replicate and averaged, with the average of mock-treated set to 100%. Error bars represent 1 SD (n = 6 for Crz1, Rod1 and Ubx7, n = 4 for Tda1). (D) Electrophoretic mobility changes in mock-treated (-), CN-treated (+) or CN + PVIVIT treated (P).

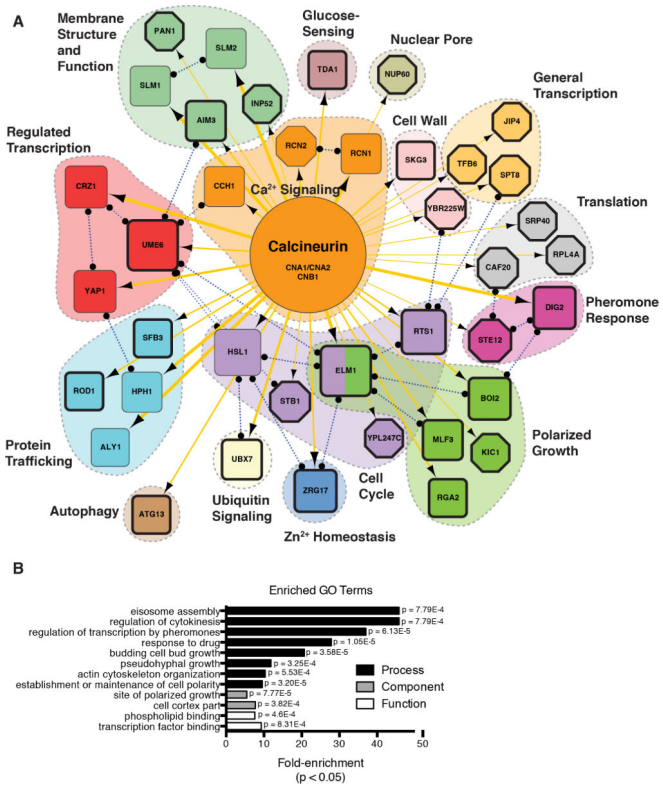

Figure 4. Characterization of the CN signaling network

(A) Gene products in CN signaling network grouped by associated cellular processes (see Table S3 and Supplemental Experimental Procedures). CN substrates (rectangles) and interacting proteins (octagons) are shown. Orange lines depict interaction with CN; line width indicates the amount of evidence supporting the interaction (see Table S3). Physical and genetic interactions between network members shown with dotted blue lines. Node size is proportional to connection number. Symbols with thick outlines designate gene products whose interaction with CN is newly identified in this study. (B) GO terms significantly enriched in the network relative to the yeast proteome. P-values of enrichment from hypergeometric distribution are shown. See also Figure S2 and Table S3.

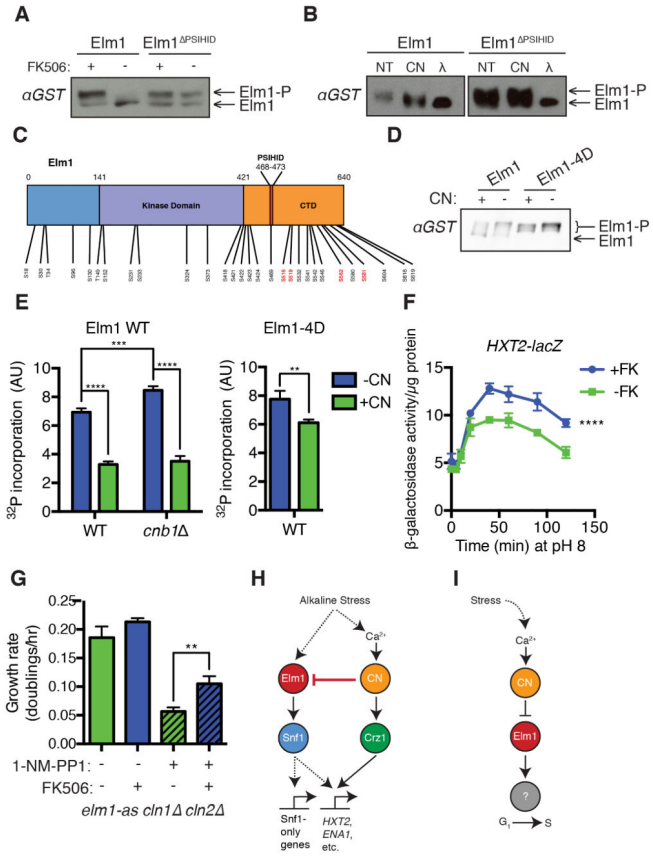

Figure 5. CN negatively regulates Elm1 activity

(A) Immunoblot analysis of extracts from CN-proficient (mock-treated, -FK) or CN-deficient (FK506-treated, +FK) yeast overexpressing GST-Elm1 or GST-Elm1$^{\Delta PSIHID}$. (B) Analysis of GST-Elm1 purified from CN-deficient yeast extracts and treated with buffer (NT), CN, or λ phosphatase (λ) *in vitro*. (C) Schematic of phosphorylation sites identified in Elm1 (see Table S1). CN-dependent dephosphorylation sites in the C-terminal domain (CTD) are shown (red) as well as the PxIxIT motif (PSIHID) (D) Immunoblot analysis of GST-Elm1 or GST-Elm1-4D (S516D, S519D, S562D, S581D) purified from WT or BY4741::*cnb1*Δ (Δ) yeast. (E) Kinase activity of GST-Elm1 or GST-Elm1-4D purified from WT or BY4741::*cnb1*Δ yeast and subsequently treated with (+CN) or without CN (-CN). ^{32}P incorporation into Snf1 substrate shown in arbitrary units (AU). Error bars are 1 SD from triplicate experiments; data analyzed by two-way ANOVA with Bonferroni post-tests. ** $p < 0.01$, *** $p < 0.001$, and **** $p < 0.0001$. (F) β-galactosidase activity of extracts from *sak1*Δ *tos3*Δ *crz1*Δ cells expressing *HXT2-lacZ* at indicated times following transfer to YPD, pH 8.0. Error bars are 1 SD from triplicate samples; data analyzed by paired, two-way ANOVA. **** $p < 0.0001$. See also Figure S3A. (G) Growth rate of *elm1-as cln1*Δ *cln2*Δ treated with 1-NM-PP1 and/or FK506. Error bars are 1 SD from triplicate samples; data analyzed by one-way ANOVA. ** $p < 0.05$. See also Figure S3B. (H) Model for dual regulation of genes by CN through Elm1 and Crz1 during alkaline stress. See also Table S4. (I) Model for regulation of Elm1 by Ca^{2+}/CN signaling during G_1.

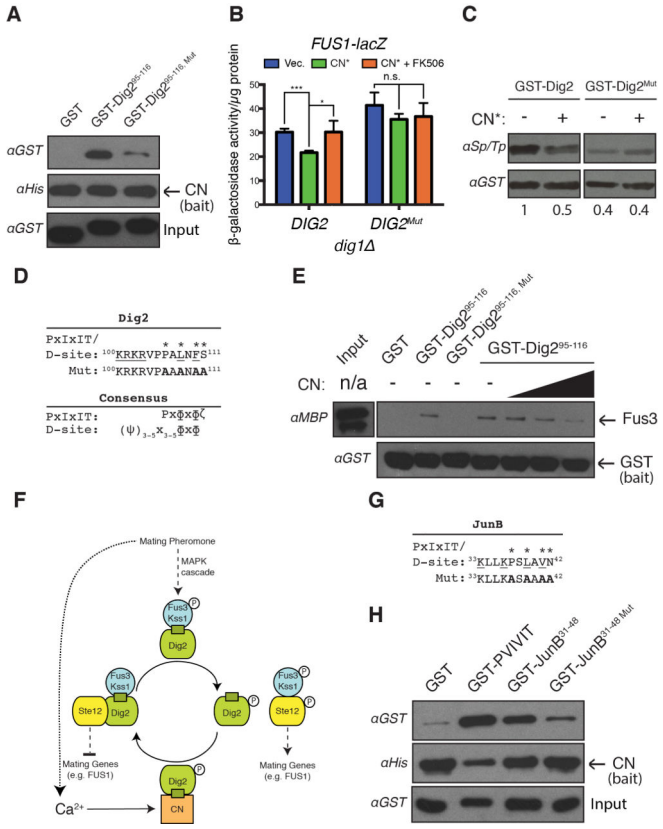

Figure 6. CN inhibits pheromone signaling by dephosphorylating Dig2 and competes with MAPK for substrate binding via overlapping docking sites

(A) Co-purification of GST or GST-Dig2$^{95\text{-}116}$ (WT or Mut, see D) with recombinant His-tagged CN (bait). (B) β-galactosidase activity of extracts from pheromone-treated *dig1*Δ cells containing *FUS1-lacZ* and *DIG2* (JRY16) or *DIG2*^{Mut} (JRY17) and expressing vector (pRS316) or constitutively active Cna1 (CN*, pCNA1trunc-316, encoding a stop codon at Ser417 to remove the calmodulin binding and autoinhibitory domains of Cna1). Cells were treated with FK506 where indicated. Error bars are 1 SD in triplicate experiments. Data analyzed by Student's T-test. * $p < 0.01$ and *** $p < 0.001$. See also Figure S4. (C) Immunoblot analysis of GST-Dig2 or GST-Dig2^{Mut} purified from extracts of pheromone-treated JRY11 cells expressing either pRS314-CNA1trunc (+CN*, constitutively active Cna1) or pRS314-CNA1 (-CN*), with α-phospho-Ser/Thr (αSpTp) and αGST antisera. Relative phosphorylation was quantified by comparing αSpTp to αGST signal and normalized to lane 1. (D) Overlapping PxIxIT/D-site in Dig2. Consensus residues in PxIxIT (*) and D-site (underlined) are shown. Key: Φ, hydrophobic residue; ζ, hydrophilic residue; Ψ, basic residue. (E) Co-purification of recombinant MBP-Fus3 with GST-Dig2$^{95\text{-}116}$ (WT or Mut, bait). CN was included in increasing amounts where indicated. (F) Model of CN-dependent regulation of Ste12-activated transcription during mating via Dig2; Ca^{2+} activates CN, which dephosphorylates Dig2 to inhibit Ste12 activity. Fus3 and CN bind competitively to Dig2 via overlapping PxIxIT/D-site (green box). (G) Overlapping PxIxIT/D-site in human JunB. (H) Co-purification of GST-tagged PVIVIT, Jun B$^{31\text{-}48}$, or Jun B$^{31\text{-}48\ Mut}$ with His-tagged human CN (bait). See also Table S2.

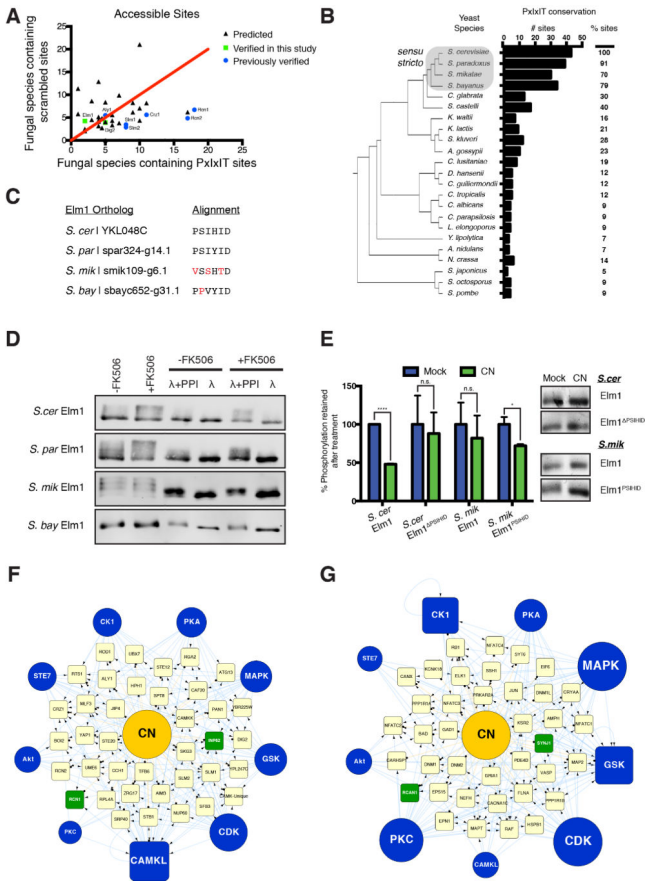

Figure 7. A Conserved set of kinase families act antagonistically to CN in yeast and mammals

(A) Conservation of PxIxIT sites in yeast CN network proteins and sequences that match the scrambled PxIxIT consensus is compared; all sites are predicted to occur in accessible protein domains. Each point represents a single protein. For proteins that contain multiple sites, the average result from all sites is plotted. Proteins with verified PxIxIT sites are labeled. Red line represents equivalent PxIxIT vs. scrambled conservation. Analysis of Rcn1 non-canonical PxIxIT site is described in supplemental experimental procedures. See also Figure S5B. (B) Tally and percentages of confirmed and putative PxIxIT sites from *S. cerevisiae* that are conserved in other fungal species. Unweighted phylogenetic tree for fungal species is shown to the left. See also Figure S5A. (C) Alignment of Elm1 PxIxIT site with corresponding regions of the homologous proteins from *sensu stricto* species. Positions that diverge from the PxIxIT consensus sequence are highlighted. See also Figure S5C. (D) Immunoblot analyses with αGST antisera of GST-tagged *sensu stricto* Elm1 proteins (Elm1-pEGH, pMMC-6, pMMC-7, pJR172), expressed in Ca^{2+}-treated BY4741 with or without FK506 treatment. Each protein was purified, then incubated *in vitro* with λ phosphatase either in the presence (λ+PPI) or absence (λ) of phosphatase inhibitors. See also Figure S5D-E. (E) *In vitro* dephosphorylation of GST-Elm1 orthologs purified from BY4741::*cnb1*Δ and processed as in Figure 3A. *S. cer* Elm1 and $Elm1^{\Delta PSIHID}$ are *S. cerevisiae* proteins containing or lacking the CN docking site. *S. mik* Elm1 and $Elm1^{PSIHID}$ are *S. mikatae* proteins containing either residues VSSHTD or PSIHID at positions 468-473. "% Phosphorylation retained after treatment": Normalized ^{32}P contents of CN-treated

samples were compared to their paired mock-treated samples and averaged, with the average of mock-treated set to 100%. Error bars represent 1 SD (n =3). Data were analyzed by Student's T-test. * $p < 0.01$ and **** $p < 0.0001$. Electrophoretic mobility changes of representative samples are depicted on the right. **(**F-G) Conserved kinases, grouped by family, that were significantly associated both with (F) yeast CN signaling network and (G) mammalian CN substrates. Kinase node size is proportional to its connectivity with CN substrates and interacting proteins. Nodes: CN phosphatase (orange), kinases (blue), conserved substrates (green), CN substrates and interacting proteins (rectangles). Edges: dephosphorylation (orange), phosphorylation (blue), CN targets (dot), kinase targets (arrow). See also Tables S5 and S6 for description of kinase family members and listing of specific interactions.